

Supplementary Material

Tumor-targeted hybrid protein oxygen carrier to simultaneously enhance hypoxia-dampened chemotherapy and photodynamic therapy at a single dose

Zhenyu Luo^{1, 3, ‡}, Hao Tian^{1, 2, ‡}, Lanlan Liu^{1, 3, ‡}, Zhikuan Chen^{1, 3}, Ruijing Liang¹, Ze Chen¹, Zhihao Wu¹, Aiqing Ma^{1, 2}, Mingbin Zheng^{1, 2, *}, and Lintao Cai^{1, *}

¹Guangdong Key Laboratory of Nanomedicine, Shenzhen engineering Laboratory of nanomedicine and nanoformulations, CAS Key Lab for Health Informatics, Shenzhen Institutes of Advanced Technology, Chinese Academy of Sciences, Shenzhen 518055, P. R. China

²Department of Chemistry, Guangdong Medical University, Dongguan 523808, PR China

³University of Chinese Academy of Sciences, Beijing 100049, PR China

‡ These authors contributed equally to this work.

*Correspondence and requests for materials should be addressed to L.C. (lt.cai@siat.ac.cn) and M.Z. (mb.zheng@siat.ac.cn).

Keywords: hybrid protein nanoparticle, targeted oxygen carrier, tumor hypoxia, chemotherapy, photodynamic therapy

Supplementary Figures

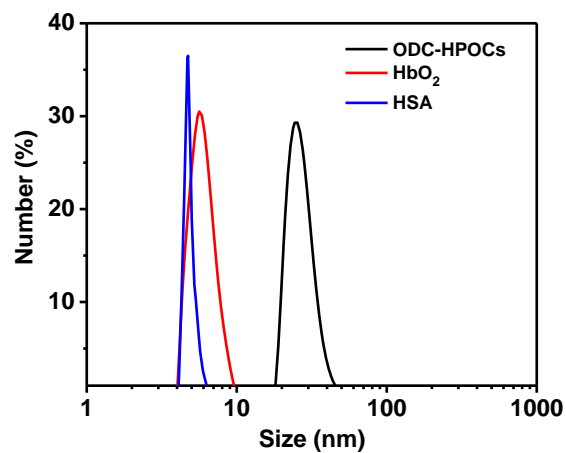


Figure S1. Size distribution of HbO₂, HSA and ODC-HPOCs.

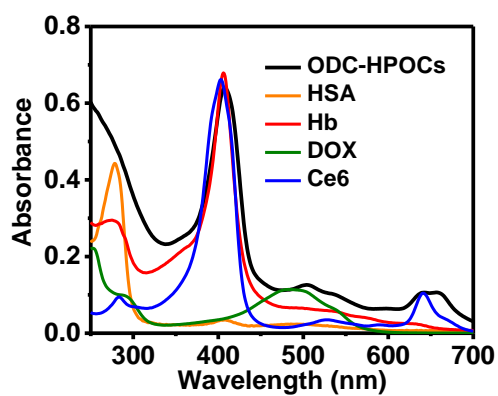


Figure S2. UV-Vis absorption spectra of ODC-HPOCs.

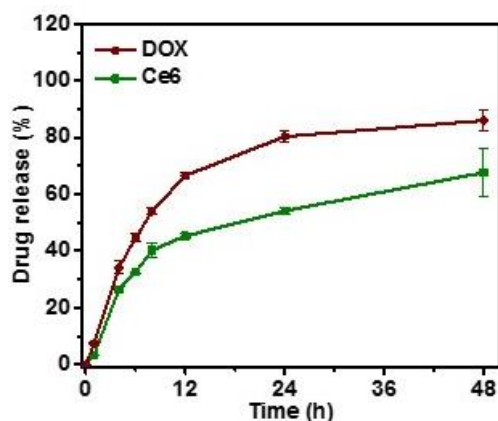


Figure S3. The releasing profiles of DOX and Ce6 in ODC-HPOCs.

Table S1. Fitting results of experimental DOX and Ce6 release data to different kinetic equations.

Samples	Kinetic model	Equation	Correlation coefficient
DOX	First-order	$y=64.6025(1-e^{-0.1064x})$	0.9658
	Higuchi	$y=13.9290x^{1/2}+4.9211$	0.8835
	Ritger-Peppas	$y=20.8482x^{0.3950}$	0.9137
Ce6	First-order	$y=85.7680(1-e^{-0.1233x})$	0.9987
	Higuchi	$y=10.8034x^{1/2}+0.5513$	0.8942
	Ritger-Peppas	$y=12.9517x^{0.4452}$	0.9034

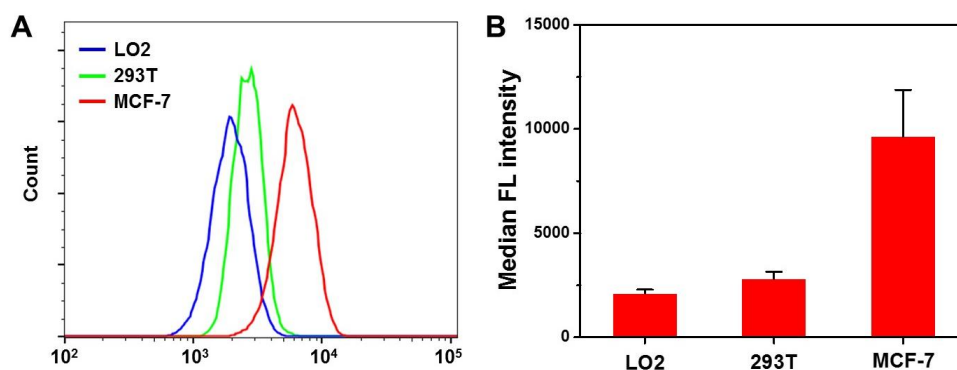


Figure S4. (A) Cellular uptake of Ce6 in cancerous (MCF-7) and normal (LO2 and 293T) cell lines after 2 h incubation with ODC-HPOCs. (B) Median fluorescent intensities of Ce6 uptake in different cells with flow cytometric analysis (Figure S4A).

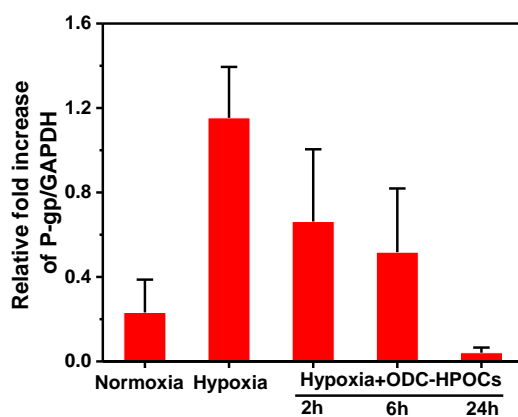


Figure S5. Semi-quantification of the P-gp expression (Figure 2D) *in vitro* (n=3).

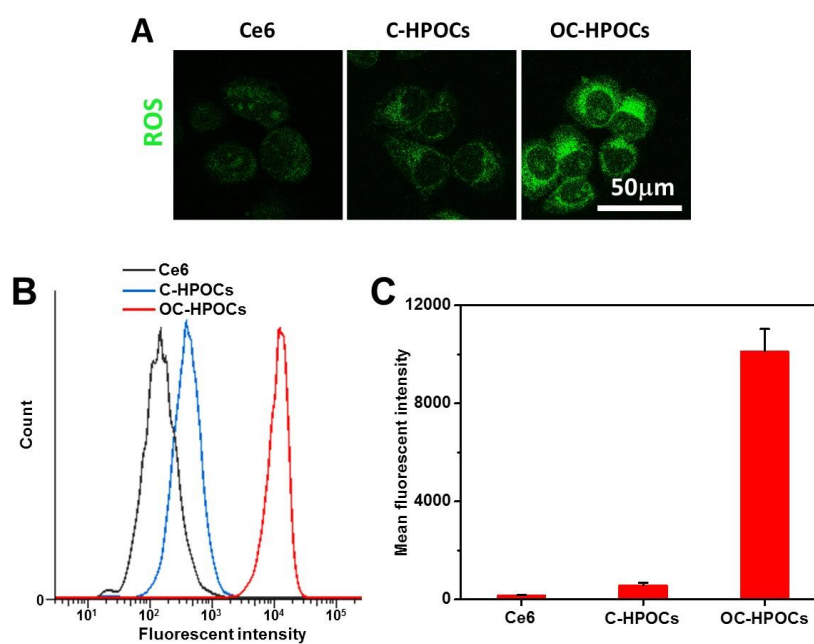


Figure S6. (A) Fluorescence imaging of ROS generation in MCF-7 cells treated with Ce6, C-HPOCs and OC-HPOCs (Ce6-encapsulated HPOCs) with laser irradiation. (B) Flow cytometric profiles of ROS generation in MCF-7 cells after PDT treatment with Ce6, C-HPOCs and OC-HPOCs. (C) Mean fluorescent intensities of ROS probe in the flow cytometric analysis (Figure S6B).

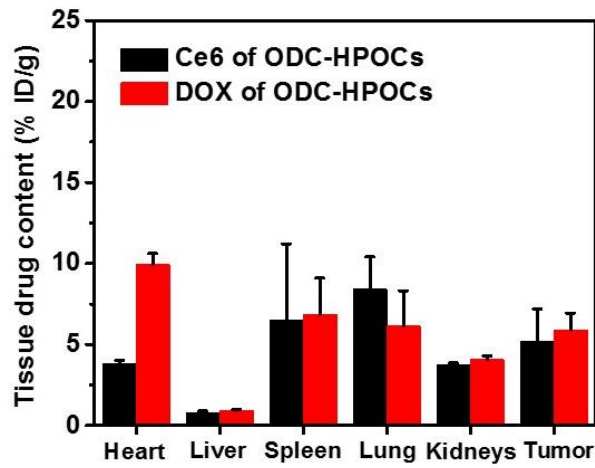


Figure S7. Quantitative biodistribution analysis of ODC-HPOCs by measuring fluorescence of Ce6 and DOX in tissue lysate (in the unit of % ID/g).

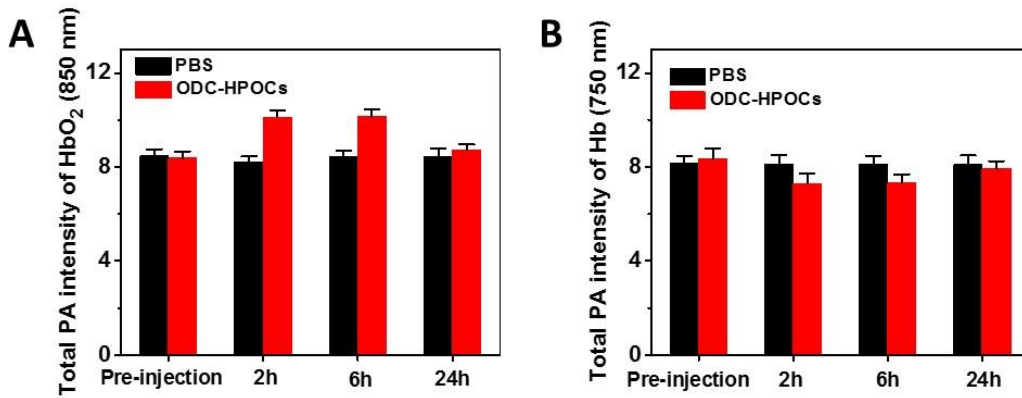


Figure S8. (A) Quantified PA intensities of HbO₂ (850 nm) around the tumor at indicated time points. (B) Quantified PA intensities of Hb (750 nm) around the tumor at indicated time points.

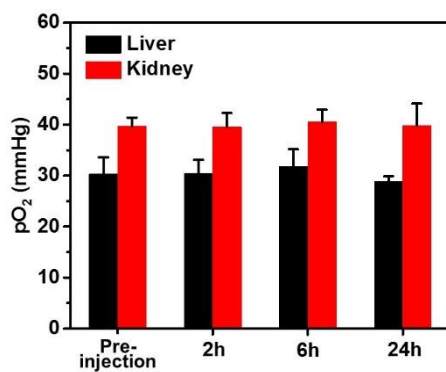


Figure S9. Measurement of pO₂ in liver and kidney by OxyLite device (Oxford Optronix, UK) after mice were intravenously injected with ODC-HPOCs.

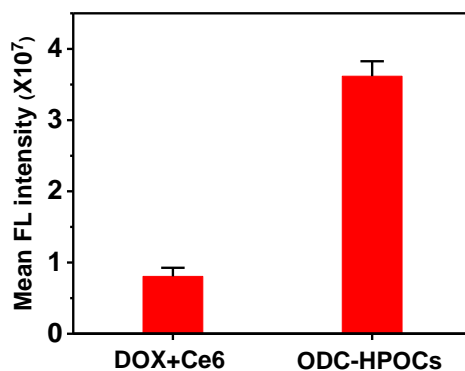


Figure S10. Quantified FL intensities of DOX around the tumor at 24h after intravenous administration of DOX+Ce6 and ODC-HPOCs, respectively.

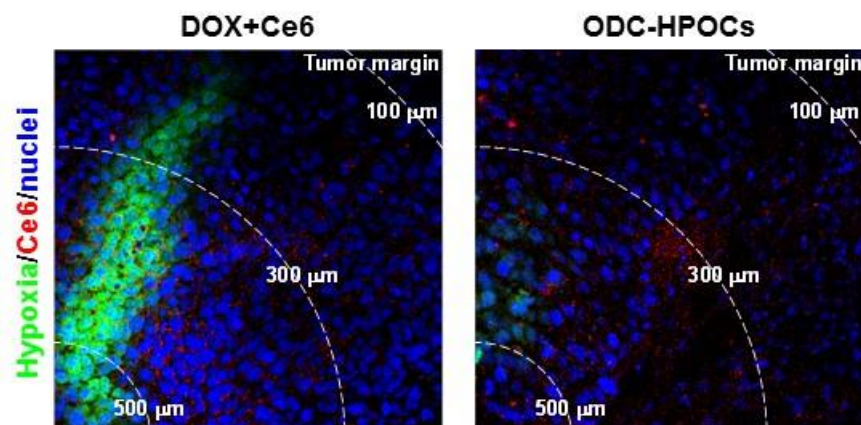


Figure S11. Distribution of hypoxia (green), Ce6 (red) and nuclei (blue) in tumor 24h after intravenous injection of DOX+Ce6 and ODC-HPOCs.

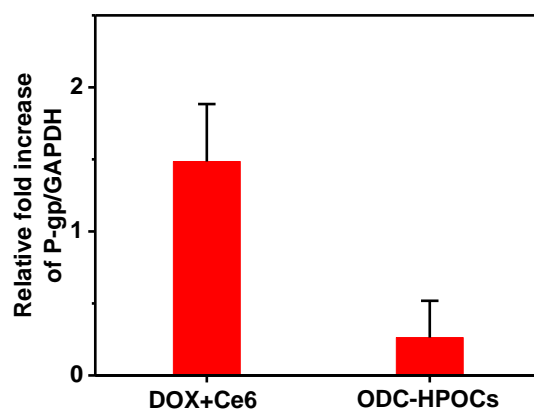


Figure S12. Semi-quantification of the P-gp expression *in vivo*.

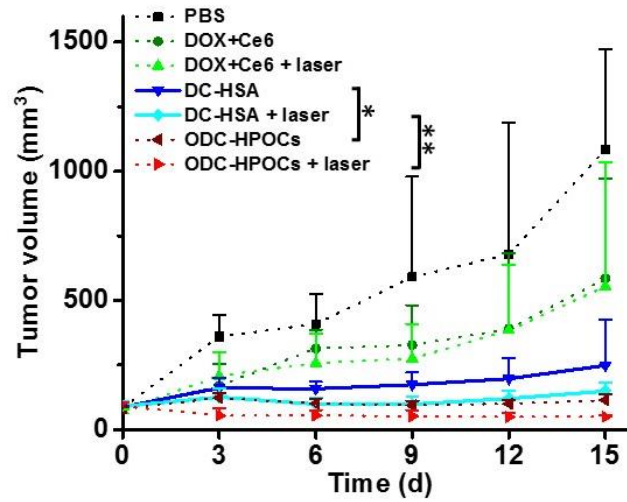


Figure S13. Tumor growth curves of DC-HSA and DC-HSA+laser. The groups of Figure 4I were added as dash lines for comparison. * $P < 0.05$, ** $P < 0.01$.

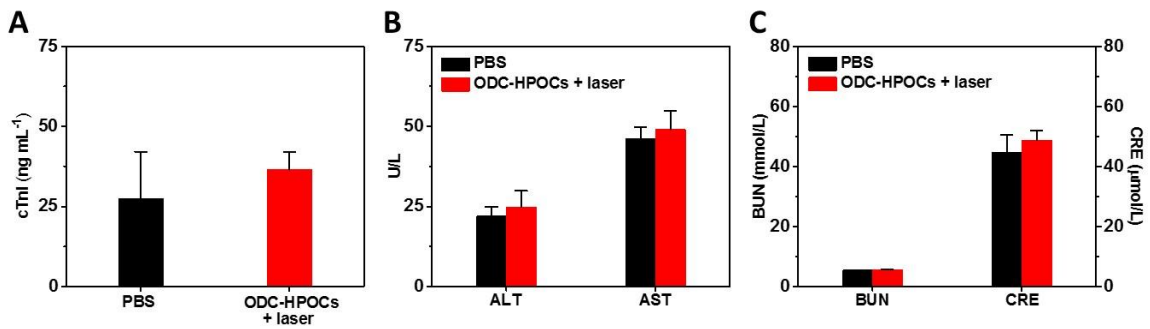


Figure S14. Serum levels of (A) cTnI (cardiac function marker), (B) ALT/AST (liver function marker) and (C) BUN/CRE (renal function marker) of mice on 15 day after different treatments (n=5).